Energy Transfer-Enabled Unsymmetrical Diamination Using Unprecedented Bifunctional Nitrogen-Radical Precursors

Authors: Guangying Tan, Mowpriya Das, Roman Kleinmans, Felix Katzenburg, Constantin Daniliuc, and Frank Glorius*

Organisch-Chemisches Institut, Westfälische Wilhelms-Universität Münster, Corrensstrasse 36, 48149 Münster, Germany.

*Correspondence to: glorius@uni-muenster.de

Abstract: Vicinal diamines, especially unsymmetrical ones, are among the most common structural motifs in biologically active molecules, natural products, and pharmaceuticals. While the catalytic diamination of carbon–carbon double bonds provides rapid access to diamines, these reactions are often limited to installing undifferentiated amino functionalities through transition-metals or hyper-valent iodine reagents catalysis. Herein, we disclose a metal-free, photosensitized dearomative unsymmetrical diamination of various electron-rich (hetero)arenes with bifunctional diamination reagents, producing a series of previously inaccessible vicinal diamines with excellent regio- and diastereoselectivity. A class of unprecedented bifunctional nitrogen-radical precursors was developed for the first time to simultaneously generate two N-centered radicals with different reactivities via an energy transfer (EnT) process. In addition, the protocol was also suitable for a wide range of alkenes. Notably, the formed vicinal diamines bear two differentiated amino functionalities, and either imine or amide units could be easily and orthogonally converted into unprotected amines, thereby facilitating the selective downstream transformations.

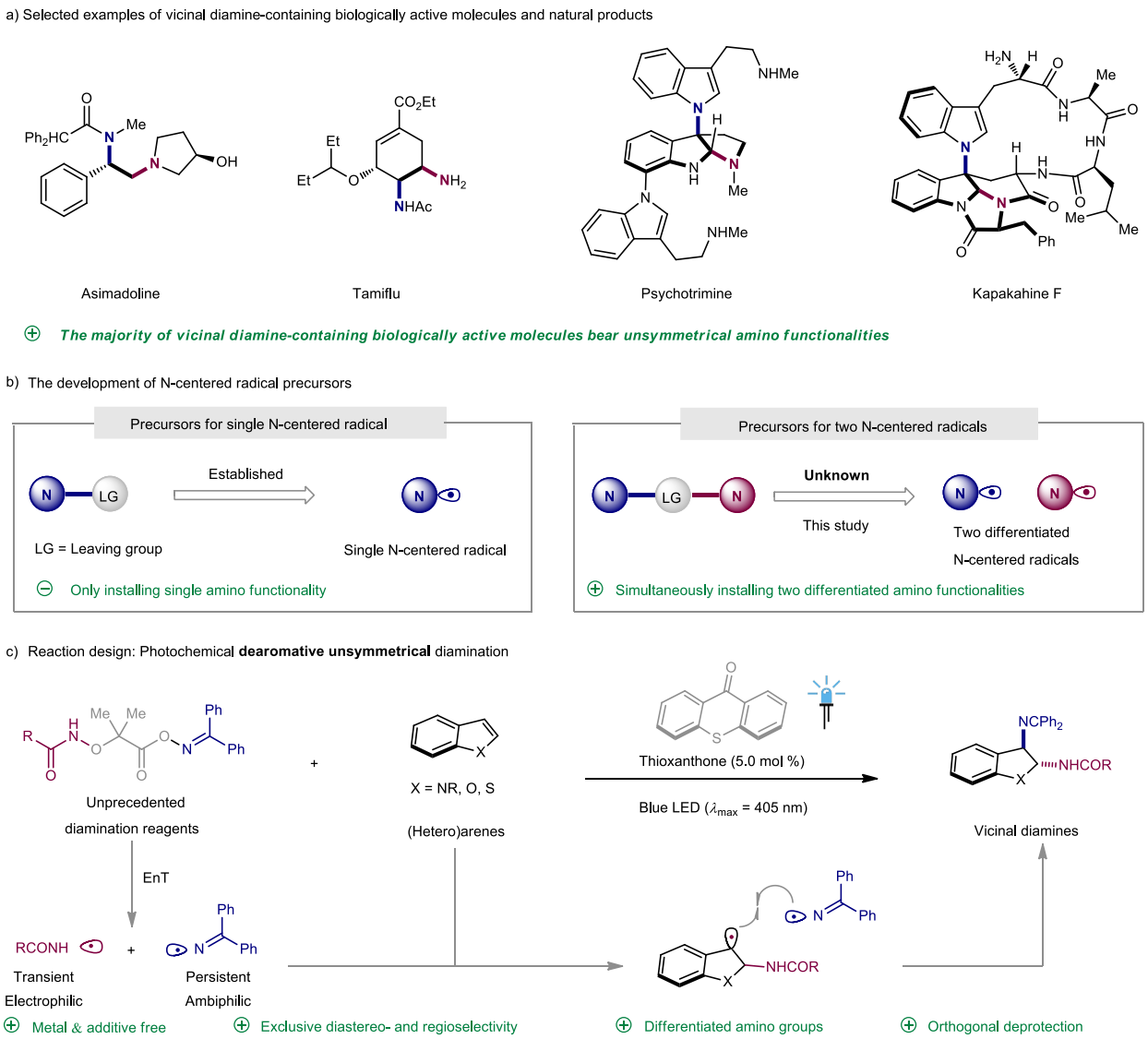

Fig. 1. Development of nitrogen-radical precursors. a) Selected examples of vicinal diamine-containing biologically active molecules, drugs, and natural products. b) The development of nitrogen-radical precursors. c) This study: Photochemical dearomative unsymmetrical diamination. EnT: energy transfer.

Vicinal diamines are the central structural motifs of a wide variety of biologically active molecules, natural products, and pharmaceuticals (Fig. 1a).[1-3] Moreover, these diamine frameworks are also frequently employed as organocatalysts, and privileged ligands for transition-metal catalysis.[4] Among various synthetic approaches to vicinal diamines, the catalytic diamination/diazidation of carbon–carbon double bonds is generally regarded as one of the most efficient and straightforward methods and has been of great interest to synthetic chemists.[5-6] Despite significant achievements made in the past few decades,[7-41] some fundamental issues still

remain to be solved in this field. First, the majority of these methods require transition-metals or hyper-valent iodine reagents as catalysts.[9-19,23-25,28,33-41] In addition, the utilization of stoichiometric amounts of metal reagents (e.g. osmium or cobalt),[7-8] chemical oxidants,[11,15,22,23,27,28,33,34,37,38] or azide reagents,[14-16,18-20,26,28,40,41] leads to the issues on cost, environment, and safety. Second, the established protocols are often limited to symmetrical diamination,[7-23,26-28] namely installing two undifferentiated amino functionalities across alkenes. From the synthetic perspective, unsymmetrical diamination is a more attractive but challenging task,[29] due to the lack of suitable amination reagents, and potential regio- and diastereoselectivity issues. Although some elegant unsymmetrical alkene diaminations have been realized,[30-41] methods to access a diamine precursor which could be easily and orthogonally converted into synthetically relevant unsymmetrical diamine products are still highly desirable.

In recent years, particularly with the bloom of visible light photocatalysis,[42-46] the N-centered radicals have received remarkable attention from synthetic community because these powerful species offer great opportunities for the construction of C–N bonds with many complementary aspects of both ionic and transition-metal-based methods in terms of retrosynthetic bond-disconnection and reaction selectivity.[47-52] So far, various nitrogen-radical precursors have been developed, and the formed radicals can be broadly divided into four classes on the basis of N-hybridization and substituents, including ambiphilic iminyl radicals, electrophilic amidyl radicals, nucleophilic aminyl radicals, and their protonated analogues, electrophilic aminium radicals.[52] Despite having received continuous progress, to the best of our knowledge, all the reported nitrogen-radical precursors are designed for producing single N-centered radicals, so they are only developed for installing single or undifferentiated amino functionalities. To realize the more challenging unsymmetrical diamination, we reasoned whether we could design a bifunctional reagent, which is in principle amenable to the simultaneous generation of two N-centered radicals at an equal rate but with different reactivities. If successful, then the regioselective stepwise addition of two differentiated N-centered radicals across carbon–carbon double bonds may provide direct access to the unsymmetrical vicinal diamines.

Herein, we report a class of unprecedented oxime ester-based bifunctional nitrogen-radical precursors to be utilized for the simultaneous generation of ambiphilic iminyl and electrophilic amidyl radicals via an energy transfer strategy,[53-55] therefore providing a rapid and versatile

protocol for unsymmetrical diamination of various electron-rich (hetero)arenes and alkenes. Noteworthy features of this method include: 1) this mild diamination reaction was performed with a cheap and commercially available thioxanthone as organic photosensitizer, without requirement of any transition-metals and additives, thus being of high practicability; 2) moreover, this protocol exhibits remarkable compatibility in dearomative diamination of a variety of (hetero)arenes, and is of exclusive diastereo- and regioselectivity, thanks to the different reactivities of iminyl and amidyl radicals; 3) most notably, the formed vicinal diamines bear two differentiated amino functionalities, and either imine or amide groups could be easily and orthogonally converted into unprotected amines, thereby facilitating the downstream transformation. Taken together, the current protocol offers a promising solution towards the main limitations of catalytic diamination.

Results and discussion

Reaction development. Considering both iminyl and amidyl radicals are two types of widely-explored N-centered radicals, showing ambiphilic and electrophilic properties,[52] respectively, our investigation commenced with the development of iminyl and amidyl-containing bifunctional nitrogen-radical precursors. As shown in Fig. 2a, various unprecedented oxime ester-based nitrogen-radical precursors were synthesized for the first time, and their reactivities were examined under visible-light-sensitized conditions by using *tert*-butyl 1*H*-indole-1-carboxylate **H1** as N-centered radical acceptor. We hypothesized that these precursors could undergo a N–O bond fragmentation through photosensitization to their triplet excited state via EnT catalysis, resulting in iminyl and amidyl radicals along with the release of CO_2 and aldehyde/ketone. Indeed, the desired dearomative diamination reactions of **H1** with a series of bifunctional nitrogen-radical precursors **S1**-**S10** were observed in the presence of a cheap and commercially available thioxanthone as photosensitizer (5.0 mol %), after irradiation for 12 h with blue LEDs (18 W, λ_{max} = 405 nm) in acetone. To our delight, the desired vicinal diamine product **8** was obtained in 72% isolated yield with excellent regio- and diastereoselectivity when employing Troc-protected bifunctional reagent **S8**. Reasonably, the monomethyl or α-unsubstituted Troc-protected bifunctional reagents **S9** and **S10** gave a reduced outcome of product **8**, likely because of the fact that the α-substituents may increase the rate of the radical decarboxylation step.[56-57] Replacement of the benzophenone iminyl with a phthalimidyl unit (**S11** and **S12**), the transformation was shut down completely, suggesting that

the benzophenone iminyl radical with a relatively long lifetime played a critical role for the dearomative diamination.[58] In order to further understand the reactivities of these bifunctional reagents, their triplet energies were determined by DFT calculation, ranging from 46.8 to 64.7 kcal mol^{-1} (Fig. 2, see Supplementary Information for the details). Given the triplet energy of thioxanthone was previously reported as 65.5 kcal mol^{-1},[59] energy transfers from thioxanthone to **S1**-**S12** are all thermodynamically feasible. To explore the lack of reactivity of **S11** and **S12**, the spin density distributions of the triplet states were determined (Fig. S14, see Supplementary Information for the details). As for both species, the spin density is predominantly localized on the phthalimide functionalities, it is expected that a high energy barrier has to be overcome to enable homolytic N–O bond breaking. In addition, the reaction of **H1** with **S8** was analyzed by GC-MS measurement to elucidate the composition of reaction mixtures (Fig. S3, see Supplementary Information for the details). **S8** was completely consumed, given its high reactivity to generate a pair of N-centered iminyl and amidyl radicals under the standard reaction conditions. The protonation of both N-centered iminyl and amidyl radicals, as well as the homo-coupling reaction of persistent N-centered iminyl radical were the main side-reactions observed in the reaction. Meanwhile, small amount of 1*H*-indole was also observed in the reaction mixtures, resulting from the deterioration of **H1**. Subsequently, the impact of other reaction parameters was also investigated (Fig. 2b). As expected, this transformation did not proceed in the absence of either thioxanthone or blue light (Fig. 2b, entries 1-2). Satisfactorily, product **8** could be obtained in 48% yield when reducing the loading of thioxanthone to 1.0 mol % (Fig. 2b, entry 3). The reaction appeared to be less sensitive to the solvents, as replacing acetone with EtOAc, CH_2Cl_2, or THF as solvent still furnished **8** in moderate to good yields (Fig. 2b, entries 4-6). Moreover, different photocatalysts were screened, and the $[Ir(dF(CF_3)ppy)_2(dtbbpy)](PF_6)$ complex was also proven to be a suitable catalyst for this dearomative diamination without diminishing the outcome. Furthermore, screening of the ratio of **H1** and **S8** were conducted under the standard conditions (Table S2, see Supplementary Information for the details). Either reducing the dosage of **H1** or switching the stoichiometry of **H1** and **S8** led to diminished yields of **8** (Table S2, entries 1-5), likely because of the deterioration of **H1** in the reaction. Finally, a conditions-based sensitivity screening suggested that this protocol was less sensitive towards the concentration of substrates, moisture, and scale-up, only suffering from slightly diminished yields at high oxygen concentration or low light intensity (see Supplementary Information for the details).[60]

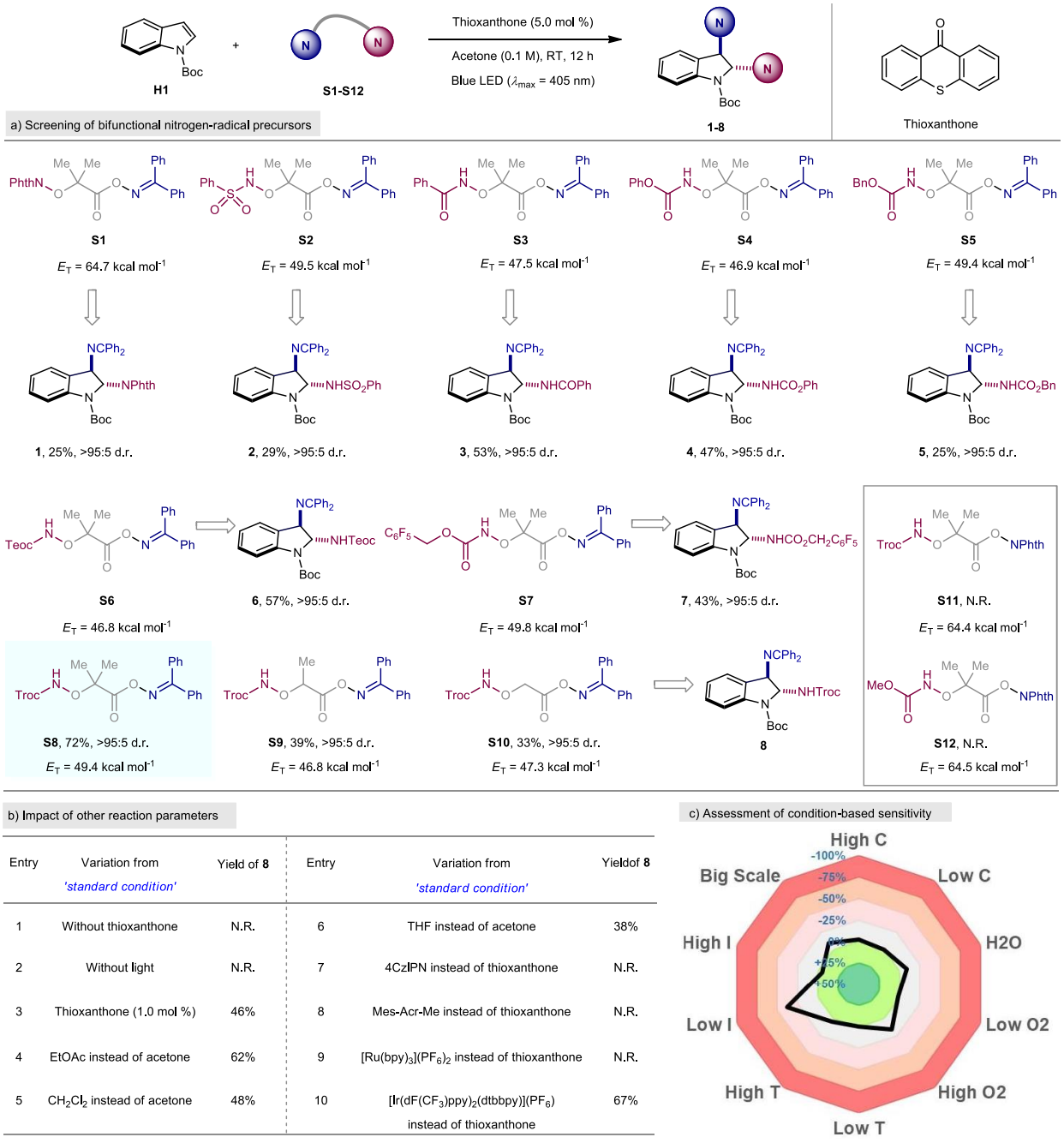

b) Impact of other reaction parameters

Entry	Variation from 'standard condition'	Yield of **8**	Entry	Variation from 'standard condition'	Yield of **8**
1	Without thioxanthone	N.R.	6	THF instead of acetone	38%
2	Without light	N.R.	7	4CzIPN instead of thioxanthone	N.R.
3	Thioxanthone (1.0 mol %)	46%	8	Mes-Acr-Me instead of thioxanthone	N.R.
4	EtOAc instead of acetone	62%	9	$[Ru(bpy)_3](PF_6)_2$ instead of thioxanthone	N.R.
5	CH_2Cl_2 instead of acetone	48%	10	$[Ir(dF(CF_3)ppy)_2(dtbbpy)](PF_6)$ instead of thioxanthone	67%

c) Assessment of condition-based sensitivity

Fig. 2. Reaction development. a) Screening of bifunctional nitrogen-radical precursors. Reaction conditions: **H1** (0.4 mmol), **S1-S12** (0.2 mmol), and thioxanthone (5.0 mol %) in acetone (0.1 M), irradiation with an 18 W blue LED (λ_{max} = 405 nm) under Ar at room temperature for 12 h. Isolated yields are given. The d.r. values were determined by ^{1}H NMR analysis. b) Impact of other reaction parameters. c) Assessment of condition-based sensitivity. Boc: *tert*-butoxycarbonyl. PhthN: phthalimidyl. Teoc: 2-(trimethylsilyl)ethoxycarbonyl. Troc: 2,2,2-trichloroethoxycarbonyl.

Mechanistic investigations. To get some insights into this dearomative diamination, a series of mechanistic studies were performed. Firstly, the reaction of **H1** and **S8** was completely inhibited

by adding 2.0 equivalent of TEMPO as a radical scavenger, and the TEMPO-adduct **9** and radical-radical cross-coupled product **10** were detected by HRMS measurement, and products **11-13** were observed as the major byproducts by GC-MS measurement (Fig. S9 and S10, see Supplementary Information for the details). These results clearly hinted towards the radical nature of the reaction, and also demonstrated the generation of iminyl and amidyl radicals (Fig. 3a). Secondly, the reaction of **S8** with **A38** under standard conditions formed a cyclic product **14** in 22% yield, further suggesting the involvement of two N-centered radicals (Fig. 3b). Subsequently, product **8** could be obtained in 36% yield when the reaction mixture of **S8** and **H1** was irradiated with a higher energy light source (λ_{max} = 365 nm) in the absence of any photocatalyst, indicating that the SET events are unlikely in this transformation (Fig. 3c). Then, UV-vis absorption spectroscopy of all reactants and their mixtures were measured, and thioxanthone was found to be the only absorbing species in the reaction near the irradiation wavelength (λ_{max} = 405 nm) (Fig. 3d). Moreover, Stern-Volmer analysis demonstrated that the luminescence emission of thioxanthone was quenched efficiently by **S8** rather than **H1**, implying that an interaction between thioxanthone and **S8** might exist in the reaction medium (Fig. 3e). To understand the nature of their interaction, comparison of some photocatalysts with different properties was conducted (Fig. 3f). As a result, yields of product **8** correlate to the triplet state energy of photocatalysts, while they are unrelated to the redox properties.[44,59] These results implied that an energy transfer (EnT) process is likely to be operative in the reaction. Furthermore, the cyclic voltammetry measurement was conducted. As shown in Fig. 3g, no obvious oxidation peak of **S8** and **H1** was observed before +1.4 V vs SCE, which suggest that these two compounds could not be oxidized by the excited state *thioxanthone ($E_{1/2}^{[PC]*/[PC]^-}$ = +1.18 V vs SCE). Similarly, no obvious reduction peak of **S8** and **H1** was observed before -1.5 V vs SCE, which means that these two compounds could not be reduced by the *thioxanthone ($E_{1/2}^{[PC]^+/[PC]*}$ = -1.11 V vs SCE). Therefore, the thermodynamic feasibility of a single electron transfer (SET) reduction of **S8** by the excited thioxanthone was also excluded by means of the cyclic voltammetry measurement (Fig. 3g).

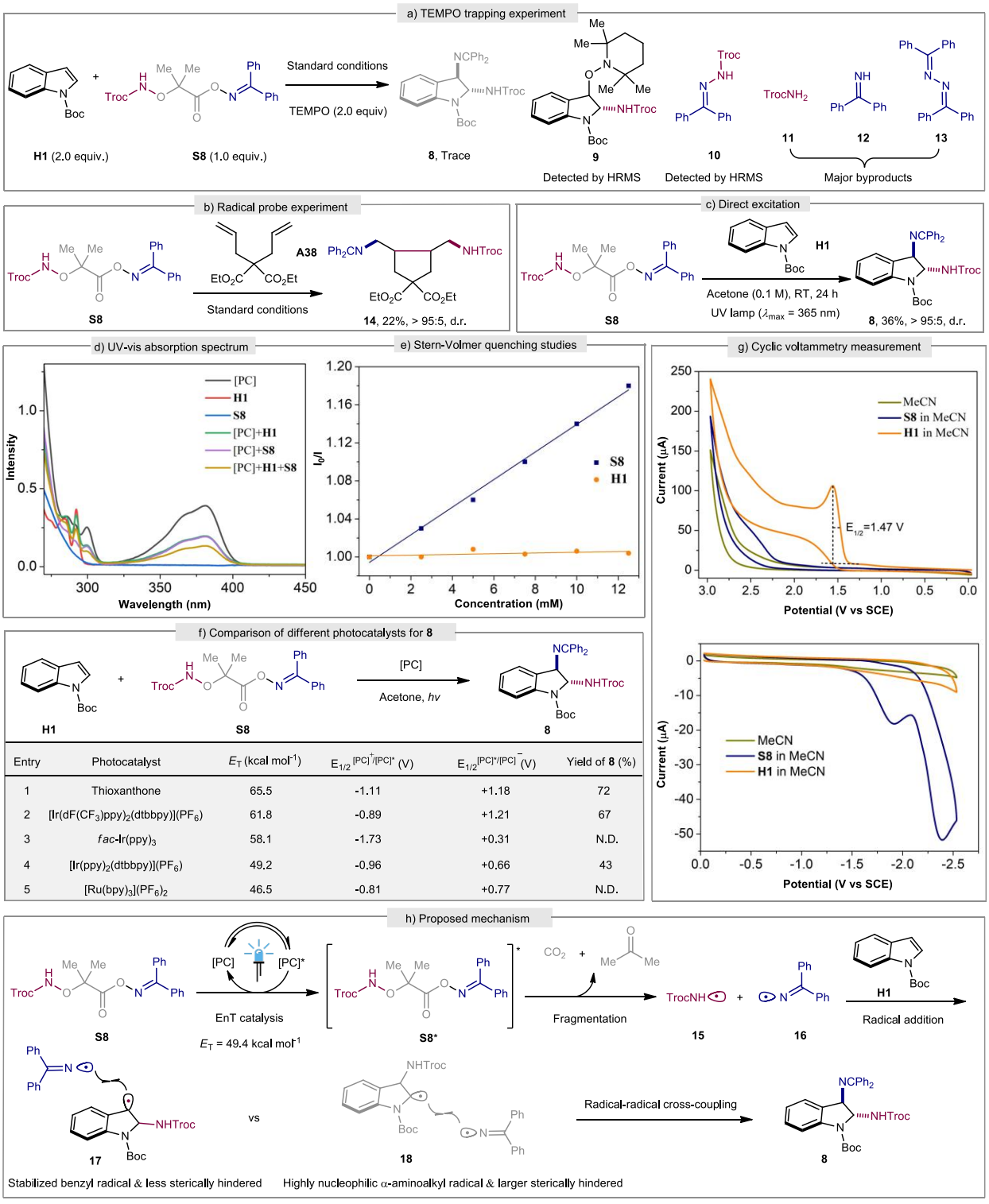

Fig. 3. Mechanistic investigations. a) TEMPO trapping experiment. b) Radical probe experiment. c) Direct excitation. d) UV-vis absorption spectrum. e) Stern-Volmer quenching studies. f) Comparison of different photocatalysts for **8**. g) Cyclic voltammetry measurement. h) Proposed mechanism. TEMPO: 2,2,6,6-tetramethylpiperidinooxy.

Taking the above results together, a plausible mechanism is proposed as outlined in Fig. 3h. The reaction starts with an interaction between **S8** and the excited thioxanthone through a photo-induced EnT process to generate the excited **S8***. The triplet energy of **S8** is computed to be 49.4 kcal mol^{-1}, which is sufficient to undergo TTEnT (triplet-triplet energy transfer) with an excited thioxanthone (E_T = 65.5 kcal mol^{-1}). Then, **S8*** undergoes a N–O bond fragmentation to form a transient amidyl radical and a persistent iminyl radical (species **15** and **16**) along with the release of CO_2 and acetone. Based on the persistent radical effect,[61-62] the electrophilic amidyl radical **15** is captured by **H1** at the C2 position to produce a transient C-centered radical **17**, followed by a radical-radical coupling process with the ambiphilic iminyl radical **16** from the opposite, sterically accessible side to produce the desired *trans*-diamine **8**. We speculated that the observed regioselectivity of this reaction might be mainly guided by the stability, electronic property, as well as steric hindrance of the generated C-centered radical after the addition of the N-centered amidyl radical to **H1**. The addition to **H1** at the C2 position generated a stabilized benzyl radical (**17**), while the addition at the C3 position would yield a highly nucleophilic α-aminoalkyl radical (**18**). Although C3 is relatively more nucleophilic than C2, the polar match of ambiphilic N-centered iminyl radical with stabilized benzyl radical (**17**) might be higher than that with highly nucleophilic α-aminoalkyl radical (**18**). Moreover, the steric hindrance of the generated C-centered radical undoubtedly played an important role in regiocontrol. Clearly, radical **17** was less sterically hindered than radical **18**, facilitating the radical-radical cross-coupling of C-centered radical with N-centered iminyl radical to furnish the desired diamine product. Notably, while **17** is a nucleophilic and relatively stabilized benzyl radical, the radical-radical cross-coupling of **17** with the electrophilic amidyl radical **15** was not observed in the reaction (Fig. S4).

Reaction scope. After investigating the reaction mechanism, the scope of this dearomative diamination was systematically investigated by using bifunctional reagent **S8** as N-centered radical source under the optimized reaction conditions. As shown in Fig. 4, a range of representative electron-rich (hetero)arenes, such as indoles, benzofurans, benzothiophenes, phenanthrene and anthracene, smoothly underwent this protocol to form a variety of unsymmetrical diamines in moderate to good yields. Indoles with different N-protection groups, such as *tert*-butoxycarbonyl (Boc), methoxycarbonyl, pivaloyl, sulfonyl, or benzoyl, reacted with **S8** in satisfactory yields (Fig. 4a, **8**, **19**-**22**), and the structure of product **21** was further

confirmed by X-ray crystallography. Then, various *N*-Boc protected indoles bearing either electron-donating or electron-withdrawing substituents on the aromatic ring or C3 position were well compatible with this reaction (Fig. 4a, **23**-**40**). Especially sensitive functional groups, such as chloro, bromo, acyloxy, ester, amide, cyano, formyl, and even boronic ester, were well-tolerated under the optimized conditions. To further test the compatibility of this method in more structurally complex contexts, several complicated indole-containing biologically active compounds such as Boc-protected Z-Trp-OMe and indoles embedded in gemfibrozil or dehydrocholic acid, were tested, affording the corresponding diamines in moderate yields (**41**-**43**). Unprotected indoles and N-alkyl or N-aryl indoles were, however, not suitable for this protocol. For instance, the reaction of 1*H*-indole **H27** with **S8** did not give any desired diamine product. The reactions of **S8** with 1-methyl-1*H*-indole **H28** or 3-methyl-1-phenyl-1*H*-indole **H29** did not deliver any diamines, neither. Instead, the C–H amidation products **44** and **45**, resulting from the re-aromatization after the addition of N-centered amidyl radical to indoles, were obtained in 16% and 15% yields, respectively. These results suggested that the electron withdrawing group at the indole N atom is indispensable for the dearomative diamination. We speculated that the electron withdrawing group at the indole N atom might decrease the nucleophilicity of C-centered benzyl radical, thereby improving the polar match with ambiphilic N-centered iminyl radiacal. This ultimately facilitated the reaction to proceed smoothly toward the desired dearomative diamination rather than the rearomative C–H amidation. In addition, the protocol could be smoothly extended to various benzofurans including xanthotoxin (Fig. 4b, **46**-**55**), as well as benzothiophenes (Fig. 4c, **56**-**58**). Surprisingly, conjugated arenes, such as phenanthrene and anthracene, despite with lower reactivity, were also found suitable for this transformation, forming the products in decent yields (Fig. 4d, **59**-**60**). Most notably, high diastereoselectivity was obtained within these diamination reactions because the stepwise addition of amidyl and iminyl radicals across carbon–carbon bonds proceeded from the opposite, sterically accessible side, producing a series of cyclic *trans*-diamines.

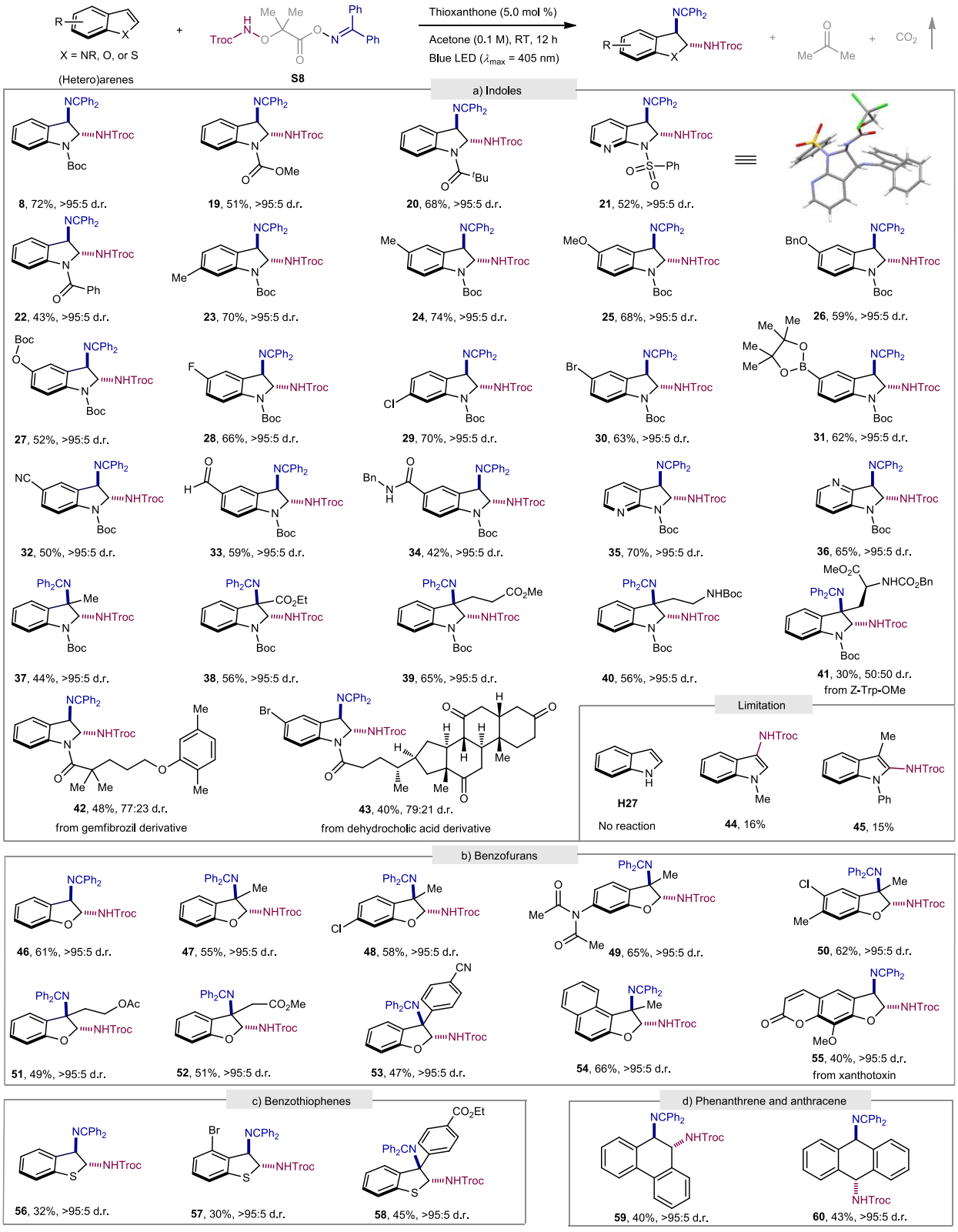

Fig. 4. Dearomative unsymmetrical diamination of (hetero)arenes. Reaction conditions: (hetero)arenes (0.4 mmol), **S8** (0.2 mmol), and thioxanthone (5.0 mol %) in acetone (0.1 M),

irradiation with an 18 W blue LED (λ_{max} = 405 nm) under Ar at room temperature for 12 h. Isolated yields are given. The d.r. values were determined by ^{1}H NMR analysis.

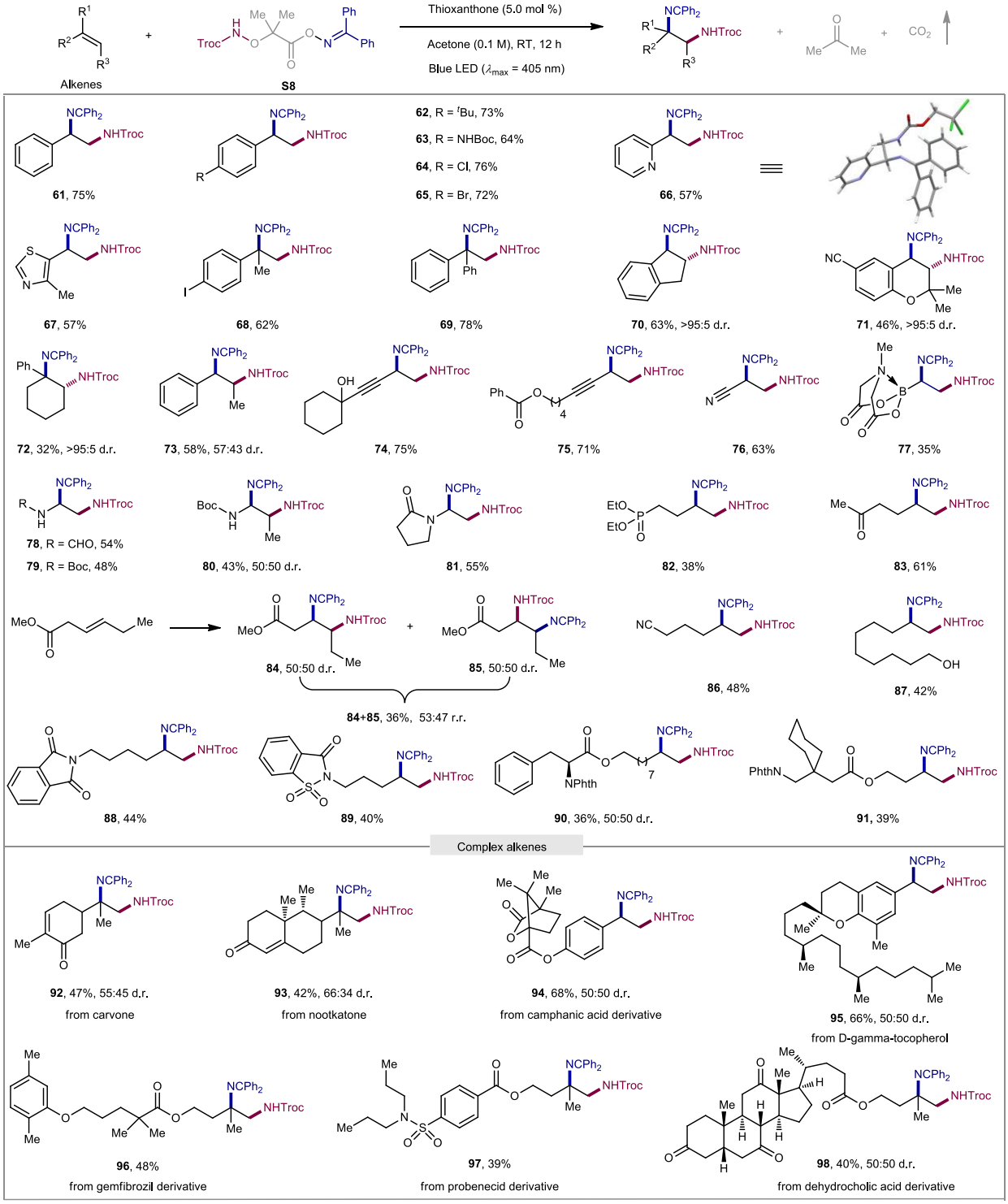

Fig. 5. Unsymmetrical diamination of alkenes. Reaction conditions: alkenes (0.4 mmol), **S8** (0.2 mmol), and thioxanthone (5.0 mol %) in acetone (0.1 M), irradiation with an 18 W blue

LED (λ_{max} = 405 nm) under Ar at room temperature for 12 h. Isolated yields are given. The d.r. values were determined by ^{1}H NMR analysis.

Then, the applicability of this method towards alkene substrates was examined as well. As summarized in Fig. 5, a wide range of alkenes, ranging from styrenes, cyclic alkenes, enynes, electron-poor or rich alkenes, to even unactivated alkenes could participate in the reaction (**61**-**98**), delivering the corresponding unsymmetrical diamines in moderate to good yields and with excellent regioselectivity. It is of note that acyclic 1,2-disubstituted alkenes were also suitable for this reaction. For example, (*E*)-prop-1-en-1-ylbenzene and (*E*)-*tert*-butyl prop-1-en-1-ylcarbamate smoothly underwent the reaction, affording the corresponding products **73** (57:43 d.r.) and **80** (50:50 d.r.) in 58% and 43% yields, respectively. Moreover, (*E*)-methyl hex-3-enoate reacted with **S8** to give an inseparable diastereoisomeric (50:50 d.r.) and regioisomeric (53:47 r.r.) mixture (**84** and **85**) in 36% total yield. Finally, the synthetic application of this protocol was further highlighted by the reaction of **S8** with complex alkenes (**92**-**98**), including the alkene-containing natural products such as carvone (**92**) and nootkatone (**93**), as well as those derived from camphanic acid (**94**), D-gamma-tocopherol (**95**), gemfibrozil (**96**), probenecid acid (**97**), and dehydrocholic acid (**98**).

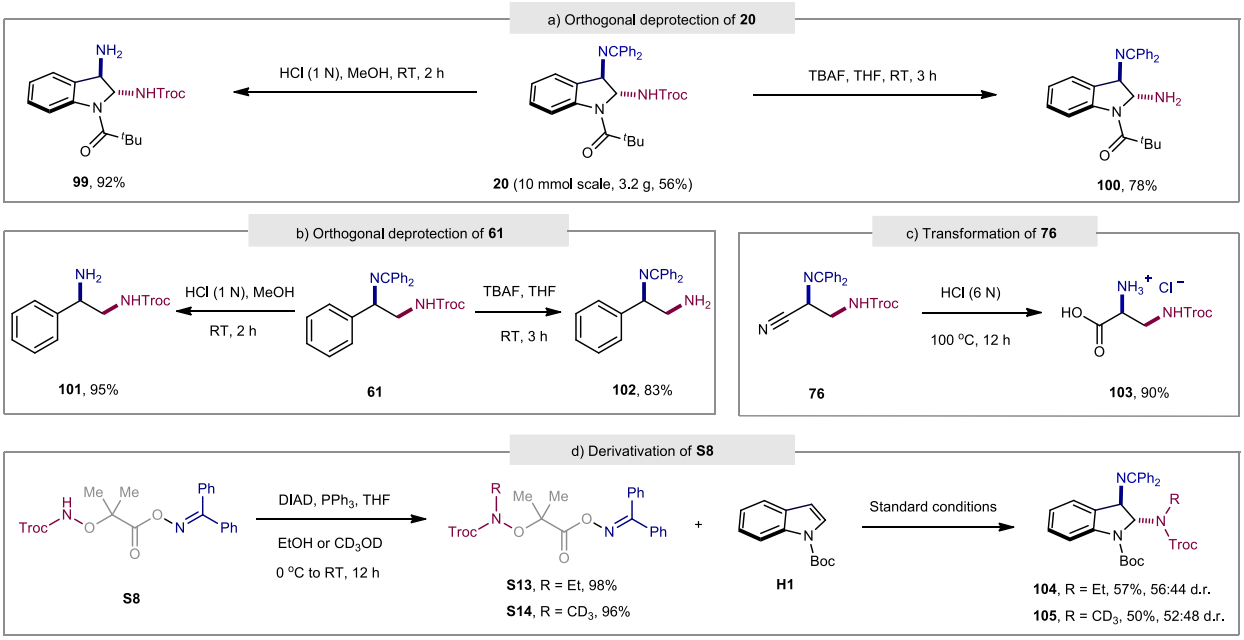

Fig. 6. Synthetic applications. a) Orthogonal deprotection of **20**. b) Orthogonal deprotection of **61**. c) Transformation of **76**. d) Derivativation of **S8**. TBAF: *tetra*-*n*-butylammonium fluoride. DIAD: diisopropyl azodicarboxylate.

Subsequently, to highlight the synthetic usefulness of this method, a 10 mmol scale reaction of **H3** with **S8** was performed under the standard reaction conditions, providing 3.2 gram of product **20** in 56% yield (Fig. 6a). Moreover, either imine or amide units on compound **20** were orthogonally deprotected under mild conditions to give the corresponding unprotected amines (**99** and **100**),[63] thereby facilitating the downstream transformation. Similarly, the orthogonal deprotections of product **61** were conducted (Fig. 6b, **101** and **102**). Thus, this protocol offers a general access to diamine precursors which could be selectively converted into synthetically relevant unsymmetrical diamine products. Additionally, treatment of product **76** with HCl (6 N) at 100 ^{o}C for 12 h generated a valuable 1,2-diamino acid **103** (Fig. 6c). Finally, N-alkyl substituted bifunctional nitrogen-radical precursors **S13** and **S14** were easily prepared through Mitsunobu reaction of **S8** with EtOH or CD_3OD in excellent yields.[64] To our delight, **S13** and **S14** smoothly underwent this reaction, producing the desired diamines in moderate yields (**104** and **105**). These results further extended the scope of bifunctional nitrogen-radical precursors, and highlighted the practicality of this method.

Conclusions

In summary, we have demonstrated a photosensitized dearomative unsymmetrical diamination of various electron-rich (hetero)arenes that is highly regio- and diastereoselective and runs under mild and transition-metal- and additive-free conditions. The developed bifunctional nitrogen-radical precursors were unprecedented, and were elaborately designed for this transformation to simultaneously generate two N-centered radicals with different reactivities via an energy transfer process. In addition, the protocol was also applicable to a wide range of alkenes. Notably, the formed vicinal diamines bear two differentiated amino functionalities, and either imine or amide units could be easily and orthogonally converted into unprotected amines, thereby facilitating the downstream transformation. We believe that this method represents an operationally simple, effective, and practical route to unsymmetrical vicinal diamines in both academic research and industry.

Acknowledgments

We thank Peter Bellotti, Dr. Xiaoye Yu, Dr. Xiaolong Zhang (all WWU), and Hyeyun Keum (KAIST) for helpful assistance and discussion.

Funding: Generous financial support by the Alexander von Humboldt Foundation (G.T.), Fonds der Chemischen Industrie (R.K., Kekulé Scholarship no. 106151), and the Deutsche Forschungsgemeinschaft (SFB 858) is gratefully acknowledged.

Author contributions: F.G. and G.T. conceived the project. G.T. and R.K. performed the initial screening experiments. G.T. and M.D. performed the synthetic experiments. F.K. conducted the computations. C.D. analyzed the X-ray structures. G.T. and F.G. supervised the research and wrote the manuscript with contributions from all authors.

Competing interests: The authors declare no competing interests.

Data and materials availability: Materials and methods, experimental procedures, mechanistic studies, computational studies, sensitivity assessment and NMR spectra are available in the Supplementary Information. CIF crystallographic data files and xyz coordinates of the optimized structures are available as Supplementary Files. Crystallographic data for the structures reported in this Article have been deposited at the Cambridge Crystallographic Data Centre, under deposition numbers CCDC 2145161 (**21**) and 2145162 (**66**). Copies of the data can be obtained free of charge via https://www.ccdc.cam. ac.uk/structures/.

References

1. Ricci, A. *Amino group chemistry: from synthesis to the life sciences*. (Wiley, 2008).

2. Lucet, D., Le Gall, T. & Mioskowski, C. The chemistry of vicinal diamines. *Angew. Chem. Int. Ed.* **37**, 2580–2627 (1998).

3. Newhouse, T., Lewis, C. A., Eastman, K. J. & Baran P. S. Scalable total syntheses of N-linked tryptamine dimers by direct indole-aniline coupling: psychotrimine and kapakahines B and F. *J. Am. Chem. Soc.* **132**, 7119−7137 (2010).

4. Kizirian, J.-C. Chiral tertiary diamines in asymmetric synthesis. *Chem. Rev.* **108**, 140–205 (2008).

5. Cardona, F. & Goti, A. Metal-catalysed 1,2-diamination reactions. *Nat. Chem.* **1**, 269–275 (2009).

6. Jong, S. de, Nosal, D. G. & Wardrop, D. J. Methods for direct alkene diamination, new & old. *Tetrahedron* **68**, 4067–4105 (2012).

7. Chong, A. O., Oshima, K. & Sharpless, K. B. Synthesis of dioxobis(*tert*-alkylimido)osmium(VIII) and oxotris(*tert*-alkylimido)osmium(VIII) complexes. Stereospecific vicinal diamination of olefins. *J. Am. Chem. Soc.* **99**, 3420–3426 (1977).

8. Becker, P. N., White, M. A. & Bergman, R. G. A new method for 1,2-diamination of alkenes using cyclopentadienylnitrosylcobalt dimer/NO/$LiAlH_4$. *J. Am. Chem. Soc.***102**, 5676–5677 (1980).

9. Bar, G. L. J., Lloyd-Jones, G. C. & Booker-Milburn, K. I. Pd(II)-catalyzed intermolecular 1,2-diamination of conjugated dienes. *J. Am. Chem. Soc.* **127**, 7308−7309 (2005).

10. Zhao, B., Du, H., Cui, S. & Shi, Y. Synthetic and mechanistic studies on Pd(0)-catalyzed diamination of conjugated dienes. *J. Am. Chem. Soc.* **132**, 3523−3532 (2010).

11. Röben, C., Souto, J. A., González, Y., Lishchynskyi, A. & Muñiz, K. Enantioselective metal-free diamination of styrenes. *Angew. Chem. Int. Ed.* **50**, 9478−9482 (2011).

12. Zhao, B. *et al.* Cu(I)-Catalyzed diamination of Conjugated dienes. Complementary regioselectivity from two distinct mechanistic pathways involving Cu(II) and Cu(III) species. *J. Am. Chem. Soc.* **133**, 20890−20900 (2011).

13. Zhu, Y., Cornwall, R. G., Du, H., Zhao, B. & Shi, Y. Catalytic diamination of olefins via N–N bond activation. *Acc. Chem. Res.* **47**, 3665–3678 (2014).

14. Fumagalli, G., Rabet, P. T. G., Boyd, S. & Greaney, M. F. Three-component azidation of styrene-type double bonds: light-switchable behavior of a copper photoredox catalyst. *Angew. Chem. Int. Ed.* **54**, 11481–11484 (2015).

15. Yuan, Y.-A., Lu, D.-F., Chen, Y.-R. & Xu, H. Iron-catalyzed direct diazidation for a broad range of olefins. *Angew. Chem. Int. Ed.* **55**, 534–538 (2016).

16. Fu, N., Sauer, G. S., Saha, A., Loo, A. & Lin, S. Metal-catalyzed electrochemical diazidation of alkenes. *Science* **357**, 575–579 (2017).

17. Muñiz, K., Barreiro, L., Romero, R. M. & Martínez, C. Catalytic asymmetric diamination of styrenes. *J. Am. Chem. Soc.* **139**, 4354−4357 (2017).

18. Shen, S.-J., Zhu, C.-L., Lu, D.-F. & Xu, H. Iron-catalyzed direct olefin diazidation via peroxyester activation promoted by nitrogenbased ligands. *ACS Catal.* **8**, 4473−4482 (2018).

19. Fu, N., Sauer, G. S. & Lin, S. A general, electrocatalytic approach to the synthesis of vicinal diamines. *Nat. Protoc.* **13**, 1725−1743 (2018).

20. Siu, J. C., Parry, J. B. & Lin, S. Aminoxyl-catalyzed electrochemical diazidation of alkenes mediated by a metastable charge-transfer complex. *J. Am. Chem. Soc.* **141**, 2825−2831 (2019).

21. Cai, C.-Y., Shu, X.-M. & Xu, H.-C. Practical and stereoselective electrocatalytic 1,2-diamination of alkenes. *Nat. Commun.* **10**, 4953−4959 (2019).

22. Tao, Z.; Gilbert, B. B. & Denmark, S. E. Catalytic, enantioselective syn-diamination of alkenes. *J. Am. Chem. Soc.* **141**, 19161−19170 (2019).

23. Minakata, S., Miwa, H., Yamamoto, K., Hirayama, A. & Okumura, S. Diastereodivergent intermolecular 1,2-diamination of unactivated alkenes enabled by iodine catalysis. *J. Am. Chem. Soc.* **143**, 4112−4118 (2021).

24. Southgate, E. H., Pospech, J., Fu, J., Holycross, D. R. & Sarlah, D. Dearomative dihydroxylation with arenophiles. *Nat. Chem.* **8**, 922 (2016).

25. Wertjes, W. C., Okumura, M. & Sarlah, D. Palladium-catalyzed dearomative *syn*-1,4-diamination. *J. Am. Chem. Soc.* **141**, 163−167 (2019).

26. Wu, J., Dou, Y., Guillot, R., Kouklovsky, C. & Vincent, G. Electrochemical dearomative 2,3-difunctionalization of indoles. *J. Am. Chem. Soc.* **141**, 2832−2837 (2019).

27. Wang, D., Yu, H., Sun, S. & Zhong, F. Intermolecular vicinal diaminative assembly of tetrahydroquinoxalines via metal-free oxidative [4+2] cycloaddition strategy. *Org. Lett.* **22**, 2425−2430 (2020).

28. Liu, J. *et al.* Diastereoselective 2, 3-diazidation of indoles via copper(II)-catalyzed dearomatization. *Chin. Chem. Lett.* **31**, 1332–1336 (2020).

29. Wang, M.-M., Nguyen, T. V. T. & Waser, J. Diamine Synthesis via the nitrogen-directed azidation of σ- and π-C−C Bonds. *J. Am. Chem. Soc.* **143**, 11969–11975 (2021).

30. Li, G., Wei, H.-X., Kim, S. H. & Carducci, M. D. A novel electrophilic diamination reaction of alkenes. *Angew. Chem. Int. Ed.* **40**, 4277−4280 (2001).

31. Jiang, H., Nielsen, J. B., Nielsen, M. & Jørgensen, K. A. Organocatalysed asymmetric β-amination and multicomponent *syn*-selective diamination of α,β-unsaturated aldehydes. *Chem. Eur. J.* **13**, 9068–9075 (2007).

32. Simmons, B., Walji, A. M. & MacMillan, D. W. C. Cycle-specific organocascade catalysis: application to olefin hydroamination, hydro-oxidation, and amino-oxidation, and to natural product synthesis. *Angew. Chem. Int. Ed.* **48**, 4349–4353 (2009).

33. Iglesias, Á., Pérez, E. G. & Muñiz, K. An intermolecular palladium-catalyzed diamination of unactivated alkenes. *Angew. Chem. Int. Ed.* **49**, 8109−8111 (2010).

34. Martínez, C. & Muñiz, K. Palladium-catalyzed vicinal difunctionalization of internal alkenes: diastereoselective synthesis of diamines. *Angew. Chem. Int. Ed.* **51**, 7031−7034 (2012).

35. Zhang, H. *et al.* Copper-catalyzed intermolecular aminocyanation and diamination of alkenes. *Angew. Chem. Int. Ed.* **52**, 2529−2533 (2013).

36. Zhang, B. & Studer, A. Copper-catalyzed intermolecular aminoazidation of alkenes. *Org. Lett.* **16**, 1790−1793 (2014).

37. Olson, D. E., Su, J. Y., Roberts, D. A. & Du Bois, J. Vicinal diamination of alkenes under Rh-catalysis. *J. Am. Chem. Soc.* **136**, 13506–13509 (2014).

38. Ciesielski, J., Dequirez, G., Retailleau, P., Gandon, V. & Dauban, P. *Chem. Eur. J.* **22**, 9338–9347 (2016).

39. Govaerts, S. *et al.* Photoinduced olefin diamination with alkylamines. *Angew. Chem. Int. Ed.* **59**, 15021–15028 (2020).

40. Makai, S., Falk, E. & Morandi, B. Direct synthesis of unprotected 2-azidoamines from alkenes via an iron-catalyzed difunctionalization reaction. *J. Am. Chem. Soc.* **142**, 21548−21555 (2020).

41. Fan, Z., Wang, Z., Shi, R. & Wang, Y. Dirhodium(II)-catalyzed diamination reaction via a free radical pathway. *Org. Chem. Front.* **8**, 5098–5104 (2021).

42. Xuan, J. & Xiao, W.-J. Visible-light photoredox catalysis. *Angew. Chem. Int. Ed.* **51**, 6828–6838 (2012).

43. Narayanam, J. M. R. & Stephenson, C. R. J. Visible light photoredox catalysis: applications in organic synthesis. *Chem. Soc. Rev.* **40**, 102–113 (2011).

44. Prier, C. K., Rankic, D. A. & MacMillan, D. W. C. Visible light photoredox catalysis with transition metal complexes: applications in organic synthesis. *Chem. Rev.* **113**, 5322–5363 (2013).

45. Skubi, K. L., Blum, T. R. & Yoon, T. P. Dual catalysis strategies in photochemical synthesis. *Chem. Rev.* **116**, 10035–10074 (2016).

46. Stephenson, C. R. J., Yoon, T. & MacMillan, D. W. C. *Visible light photocatalysis in organic chemistry*. (Wiley, 2018).

47. Zard, S. Z. Recent progress in the generation and use of nitrogen-centred radicals. *Chem. Soc. Rev.* **37**, 1603–1618 (2008).

48. Chen, J.-R., Hu, X.-Q., Lu, L.-Q. & Xiao, W.-J. *Chem. Soc. Rev.* **45**, 2044–2056 (2016).

49. Kärkäs, M. D. Photochemical generation of nitrogen-centered amidyl, hydrazonyl, and imidyl radicals: methodology developments and catalytic applications. *ACS Catal.* **7**, 4999−5022 (2017).

50. Jackman, M. M., Cai, Y. & Castle, S. L. Recent advances in iminyl radical cyclizations. *Synthesis* **49**, 1785–1795 (2017).

51. Zhao, Y. & Xia, W. Recent advances in radical-based C–N bond formation via photo-/electrochemistry. *Chem. Soc. Rev.* **47**, 2591−2608 (2018).

52. Davies, J., Morcillo, S. P., Douglas, J. J. & Leonori, D. Hydroxylamine derivatives as nitrogen-radical precursors in visible-light photochemistry. *Chem. Eur. J.* **24**, 12154–12163 (2018).

53. Strieth-Kalthoff, F., James, M. J., Teders, M., Pitzer, L. & Glorius, F. Energy transfer catalysis mediated by visible light: principles, applications, directions. *Chem. Soc. Rev.* **47**, 7190–7202 (2018).

54. Zhou, Q.-Q., Zou, Y.-Q., Lu, L.-Q. & Xiao, W.-J. Visible-light-induced organic photochemical reactions through energy-transfer pathways. *Angew. Chem. Int. Ed.* **58**, 1586–1604 (2019).

55. Strieth-Kalthoff, F. & Glorius, F. Triplet energy transfer photocatalysis: unlocking the next level. *Chem* **6**, 1888–1903 (2020).

56. Jiang, H. & Studer, A. Amidyl radicals by oxidation of α-amido-oxy acids: transition-metal-free amidofluorination of unactivated alkenes. *Angew. Chem. Int. Ed.* **57**, 10707–10711 (2018).

57. Jiang, H., Seidler, G. & Studer, A. Carboamination of unactivated alkenes through three-component radical conjugate addition. *Angew. Chem. Int. Ed.* **58**, 16528–16532 (2019).

58. Patra, T., Das, M. Daniliuc, C. G. & Glorius, F. Metal-free, photosensitized oxyimination of unactivated alkenes with bifunctional oxime carbonates. *Nat. Catal.* **4**, 54–61 (2021).

59. Nikitas, N. F., Gkizis, P. L. & Kokotos, C. G. Thioxanthone: a powerful photocatalyst for organic reactions. *Org. Biomol. Chem.* **19**, 5237–5253 (2021).

60. Pitzer, L., Schäfers, F. & Glorius, F. Rapid assessment of the reaction-condition-based sensitivity of chemical transformations. *Angew. Chem. Int. Ed.* **58**, 8572–8576 (2019).

61. Fische, H. The persistent radical effect: a principle for selective radical reactions and living radical polymerizations. *Chem. Rev.* **101**, 3581–3610 (2001).

62. Leifert, D. & Studer, A. The persistent radical effect in organic synthesis. *Angew. Chem. Int. Ed.* **59**, 74–108 (2020).

63. Huang, C.-Y. *et al. J. Carbohydr. Chem.* **29**, 289–298 (2010).

64. Jiang, H., Yu, X., Daniliuc, C. G. & Studer, A. Three-component aminoarylation of electron-rich alkenes by merging photoredox with nickel catalysis. *Angew. Chem. Int. Ed.* **60**, 14399–14404 (2021).